Carbohydrate Polymer Technologies and Applications 2 (2021) 100150

Contents lists available at ScienceDirect

Carbohydrate Polymer Technologies and Applications

journal homepage: www.sciencedirect.com/journal/carbohydrate-polymer-technologies-and-applications

Barrier biopaper multilayers obtained by impregnation of electrospun poly (3-hydroxybutyrate-*co*-3-hydroxyvalerate) with protein and polysaccharide hydrocolloids

Beatriz Melendez-Rodriguez [a], Marie-Stella M'Bengue [a,1], Sergio Torres-Giner [a,2], Luis Cabedo [b], Cristina Prieto [a], Jose Maria Lagaron [a,*]

[a] *Novel Materials and Nanotechnology Group, Institute of Agrochemistry and Food Technology (IATA), Spanish Council for Scientific Research (CSIC), Calle Catedrático Agustín Escardino Benlloch 7, 46980 Valencia, Spain*

[b] *Polymers and Advanced Materials Group (PIMA), School of Technology and Experimental Sciences, Universitat Jaume I (UJI), Avenida de Vicent Sos Baynat s/n, 12071 Castellón, Spain*

ARTICLE INFO

Keywords:
Nanocellulose
PHBV
Additives
Multilayers
Gas barrier
Food packaging

ABSTRACT

Multilayer biopapers composed of two electrospun layers of poly(3-hydroxybutyrate-*co*-3-hydroxyvalerate) (PHBV) were impregnated, at the inner side of one of the layers, with cellulose nanocrystals (CNCs) and their composites with hydrocolloids, to develop high-barrier fully biobased structures. The study aimed for the first time at comparing the impregnation of electrospun fibers with several biopolymer solutions. Thus, neat CNCs, and CNCs mixed as a minor fraction, that is, 2 wt%, with gelatin (GE), agar (AG), xanthan gum (XG), and gum arabic (GA) were assessed in their potential to improve the barrier properties of PHBV. Glycerol plasticizer was added to the composite formulations. The impregnated electrospun multilayer mats were subsequently annealed, below the PHBV melting point, to yield continuous films by an interfiber coalescence process, so-called biopapers, and thereafter characterized to evaluate their potential for high barrier food packaging applications. The morphological characterization revealed good interlayer adhesion, more noticeably for those containing CNCs and their nanocomposites with AG and XG. From their mechanical response, it was inferred that the material behavior was governed mainly by the rigidity of the PHBV substrates, and this could not be significantly improved by impregnation with any of the various hydrocolloids. Whereas the water vapor barrier was not seen to improve in any of the samples, the barrier to the organic vapor limonene, used as a standard for aroma barrier, was however improved in the samples impregnated with AG and XG composites. Interestingly, the oxygen barrier properties were significantly improved but only by impregnation with pure CNCs. This study reports for the first time a scalable impregnation technology approach to produce fully biobased barrier multilayers.

1. Introduction

In a context of global environmental problems, a change of perspective towards the use of petroleum derived materials has been gaining relevance in recent decades. The massive production of plastics, about 360 million tons per year, in combination to their non-biodegradable nature represent a serious end-of-life management problem (Geyer, Jambeck & Law, 2017). Every year, around eight billion kilograms of plastic waste reach the oceans from the coast, being 40% of which single-use items (Commission, 2018). Thus, the use of bio-based, biodegradable, and eco-friendly polymers as substitutes for traditional petrochemical ones is becoming increasingly important.

In this regard, cellulose is of great interest due to its biodegradability and abundancy (Huber et al., 2012). Cellulose is a polysaccharide

* Corresponding author.
E-mail addresses: beatriz.melendez@iata.csic.es (B. Melendez-Rodriguez), marie-stella.m-bengue@grenoble-inp.org (M.-S. M'Bengue), storresginer@upv.es (S. Torres-Giner), lcabedo@uji.es (L. Cabedo), cprieto@iata.csic.es (C. Prieto), lagaron@iata.csic.es (J.M. Lagaron).
[1] On leave from Grenoble INP – Pagora, UGA, International School of Paper, Print Media and Biomaterials, 461 Rue de la papeterie - CS 10065 - 38402 Saint-Martin d'Hères Cedex, France.
[2] This author is currently with the Research Institute of Food Engineering for Development (IIAD), Universitat Politècnica de València (UPV), Camino de Vera s/n, 46022 Valencia, Spain.

https://doi.org/10.1016/j.carpta.2021.100150
Received 23 May 2021; Received in revised form 24 August 2021; Accepted 7 September 2021
Available online 9 September 2021

composed of β-D-glucose subunits, which is found mainly in plant cell walls, but also in the tissues of algae and in the epidermal cell membrane of tunicates. Moreover, it can also be synthesized by bacteria (Y. Zhao, Moser, Lindström, Henriksson & Li, 2017). Among the cellulose derivatives, cellulose nanomaterials (CNMs) have gained relevance based on their lack of toxicity and high-mechanical and -barrier properties (Mokhena & John, 2020). In this regard, cellulose nanocrystals (CNCs) have received significant interest due to its high surface area and aspect ratio, exceptional optical transparency, unique morphology, and the possibilities for surface modification (Trache et al., 2020). As mentioned, CNCs present high-gas barrier by forming a dense hydrogen bonded self-associated network of crystals, leading to a reduced free volume, and hence preventing the passage of gas molecules. This makes CNCs very attractive for use in food packaging structures, where they could help extending food shelf-life by reducing oxygen permeation (Ahankari, Subhedar, Bhadauria & Dufresne, 2021).

However, despite the previous advantages, CNCs possess some drawbacks for their use in food packaging applications, such as their moisture sensitivity and brittleness after dehydration (Aulin, Gällstedt & Lindström, 2010). Therefore, the use of plasticizers is considered as a good alternative to enhance CNC processability. Thus, glycerol, which has shown to improve mechanical properties such as flexibility and elasticity of polymer films (Li et al., 2018; Tong, Xiao & Lim, 2013), has been used as a plasticizer for cellulose-based materials, decreasing their stiffness and increasing their elongation at break. For instance, Xiao et al. (Xiao, Zhang, Zhang, Lu & Zhang, 2003) reported an increase in elongation at break, from 6.9 to 25.4%, in regenerated cellulose films when glycerol was added. However, glycerol also decreases the barrier properties because it intercepts the hydrogen bonding between the nanocellulose chains, facilitating the permeability of the gas molecules (Hubbe et al., 2017). Thus, a balance must be found between good plasticizing efficiency and gas barrier properties.

One feasible strategy is to combine CNCs with other high-gas-barrier biopolymers, which include proteins, such as gelatin (GE), or polysaccharides, such as agar (AG), xanthan gum (XG), and gum arabic (GA). Among them, GE is a cost-effective water-soluble protein derived from collagen (Clarke et al., 2016; Hanani, A., Roos & Kerry, 2012). It is abundant in nature and it can form films with nontoxic and biodegradable properties (Ge, Wu, Woshnak & Mitmesser, 2021). Although it presents good barrier to oxygen, it has poor mechanical strength and low water barrier (Gómez-Guillén et al., 2009). For this reason, its use in combination with plasticizers or other hydrophobic biopolymers can provide stability, resistance, flexibility, and increased water barrier (Cao, Yang & Fu, 2009). CNCs have been also used along with GE as a reinforcement strategy. For example, Santos et al. (Santos et al., 2014) reported that GE/CNC nanocomposites, plasticized with glycerol and sonicated, showed a better stiffness-to-ductility balance and a reduced water vapor permeability for CNC contents of up to 5 wt%. In another work, the incorporation of 0.5 wt% of CNCs into GE increased the tensile strength and Young's modulus of GE by 77 and 48%, respectively (Leite, Ferreira, Corrêa, Moreira & Mattoso, 2020). Alternatively, AG is a polysaccharide derived from red algae (Akshay Kumar et al., 2021). It has interesting properties, such as water solubility, biodegradability, and good strength (Kanmani & Rhim, 2014; Rhim, Wang & Hong, 2013). Moreover, AG has been used along with CNCs in different composites to obtain enhanced mechanical and barrier properties. Hence, the AG/CNC composite using glycerol as plasticizer resulted in more flexible films with 23% less WVP (Reddy & Rhim, 2014). A similar work based on AG/CNC composite films presented analogous results with increased mechanical properties and reduced WVP (Atef, Rezaei & Behrooz, 2014). These results point out the good interaction between CNCs and AG. Furthermore, XG is an extracellular polysaccharide mainly produced by the Gram-negative bacterium *Xanthomonas campestris* (Jansson, Kenne & Lindberg, 1975). It has been distinguished for its non-toxicity, thermal stability and biocompatibility properties (Kumar, Rao & Han, 2018). XG can be soluble in both cold and hot water and its films present low water vapor permeability and great mechanical properties (Guo, Ge, Li, Mu & Li, 2014). Composites made of XG/chitosan (CS) blends reinforced with CNCs showed improved mechanical performance by increasing the CNC content from 2 to 10 wt% (Madhusudana Rao, Kumar & Han, 2017). Finally, GA is an exudate from the stems and branches of *Acacia* species trees (Montenegro, Boiero, Valle, & Borsarelli, 2012). It has been largely used in the food industry as stabilizer, emulsifier, flavoring agent and thickener, but also in the pharmaceutical, cosmetic, printing, and textile industries (Verbeken, Dierckx & Dewettinck, 2003). However, its use as coating or packaging film is limited due to its lack of strength, poor barrier properties, and high hydrophilicity (Aphibanthammakit, Nigen, Gaucel, Sanchez & Chalier, 2018). For this reason, the use of CNCs as a filler has been seen as a great reinforcement in composites. As an example, Kang et al. (Kang, Xiao, Guo, Huang & Xu, 2021) reported an increase in tensile strength and elongation at break by incorporating 4 wt% CNCs into GA films as well as a 10.6 and 25.3% decrease in water vapor and oxygen permeabilities, respectively.

As cited above, since CNCs are strongly plasticized by moisture sorption (Wang et al., 2018), it can only be used, as most oxygen-barrier polymers, protected between water-barrier layers. For this reason, the use of multilayer systems where a CNC-based middle layer protected between hydrophobic polymers has been seen as a great alternative to overcome this problem (Fotie, Gazzotti, Ortenzi & Piergiovanni, 2020; Le Gars et al., 2020). Among the hydrophobic polymers available, biopolymers such as polyhydroxyalkanoates (PHAs) stand out for their biodegradability and compostability, whereas they can also be processed using conventional plastic machinery (Bhatia et al., 2021). The poly(3-hydroxybutyrate) (PHB) homopolymer and its poly(3-hydroxybutyrate-*co*-3-hydroxyvalerate) (PHBV) (Guk Choi, Woong Kim, Kim & Ha Rhee, 2003), poly(3-hydroxybutyrate-*co*-4-hydroxybutyrate) [(P3HB-*co*-P4HB)] (Torres-Giner, Montanes, Boronat, Quiles-Carrillo & Balart, 2016), poly(3-hydroxybutyrate-*co*-3-hydroxyhexanoate) [P(3HB-*co*-3HHx)] (Qiu, Han & Chen, 2006), or poly(3-hydroxybutyrate-*co*-3-hydroxyvalerate-*co*-3-hydroxyhexanoate) [P(3HB-*co*-3HV--*co*-3HHx)] (Zhang, Ma, Wang & Chen, 2009) copolymers, are the most studied PHAs since they have been used as substitutes for petrochemical polymers such as polypropylene (PP) and polyethylene (PE). In particular, PHBV has low crystallinity and moderate flexibility (Chen, Don & Yen, 2006; W. Zhao & Chen, 2007), high moisture resistance, and medium-gas-barrier properties (Gallardo-Cervantes et al., 2021).

Electrospinning, is an emerging processing technology in which the use of an electric field allows the creation of polymer micro- and nanofibers (Doshi & Reneker, 1995) and it is currently seen as a promising alternative to develop polymer layers after annealing. These layers are useful for the packaging industry since they can improve the mechanical and barrier performance of some polymers (Torres-Giner, 2011). Thus, a very short thermal post-treatment to the fibers, below their melting point, convert them into continuous films, so-called biopapers, by interfiber coalescence, exhibiting adhesive properties, improved transparency, flexibility, and barrier performance (Cherpinski, Torres-Giner, Cabedo, Méndez & Lagaron, 2018; Melendez-Rodriguez et al., 2020). For instance, electrospun PHB and PHBV coatings have already been reported to improve the moisture resistance of nanopapers based on cellulose nanofibrils (CNFs) and lignocellulose nanofibrils (LCNFs) when structured in a multilayer fashion (Cherpinski et al., 2018). In another study, coatings made of electrospun PHB/bacterial cellulose, which covered the inner layer of thermoplastic corn starch (TPCS)/bacterial cellulose composites, improved their water- and oxygen-barrier properties (Fabra, López-Rubio, Ambrosio-Martín & Lagaron, 2016). In addition, electrospun fibers can be functionalized with the use of additives with antimicrobial or antioxidant properties, which increases their application interest in active packaging applications(Figueroa-Lopez et al., 2020c) (Figueroa-Lopez et al., 2020b)(K. J. Figueroa-Lopez et al., 2020; Kelly J. Figueroa-Lopez, S. Torres-Giner, et al., 2020).

From all of the above and to the best of our knowledge, electrospun PHAs have only been used before to reduce the moisture sensitivity of previously formed nanopapers made of cellulose nanofibers (CNF). This study offers the opposite perspective, in which electrospun PHA biopapers were impregnated with CNCs and also with various hydrocolloids containing CNCs in order to improve the barrier properties, assessing whether these novel layered materials could offer advantages in biobased food packaging applications. To this end, CNCs were used alone and mixed as a minor component with a protein and various polysaccharides, adding glycerol as a plasticizer, and the mechanical and barrier properties of the resultant nanocomposite films were determined and compared to an equivalent multilayer film of neat PHBV. Therefore, the interest of the study mainly comes from the fact that, during optimal annealing post-processing, the electrospun fibers can successfully coalesce, resulting in denser thinner and continuous layers. Thus, it was uncertain if, by a simple and scalable impregnation process, an improvement in barrier properties of PHBV could be achieved.

2. Experimental

2.1. Materials

The commercial PHBV used was ENMAT Y1000P, supplied by Tianan Biologic Materials (Ningbo, China). The 3HV fraction is approximately 2 mol% and the molecular weight (M_W) is ~2.8×10^5 g/mol. CNCs were provided by CelluForce NCC® (Quebec, Canada) as pure cellulose sulfate sodium salt, which was obtained from wood pulp, and was received as a spray-dried solid white powder with a bulk density of 0.7 g/cm^3.

2,2,2-Trifluoroethanol (TFE), ≥ 99% purity, D-limonene, with 98% purity, and GE type-B from bovine skin were obtained from Sigma Aldrich S.A. (Madrid, Spain). Glycerol, pharmaceutic grade, with a density of 1.26 g/cm^3, was purchased from Panreac S.A. (Barcelona, Spain). Potato dextrose AG was supplied by Scharlab S.L. (Barcelona, Spain), whereas XG and GA were obtained from Guinama S.L. (Valencia, Spain). The chemical structures of the hydrocolloids are shown in Fig. 1.

2.2. Electrospinning process

The commercial PHBV pellets were dissolved at 10 wt% in TFE under magnetic stirring for 24 h at 50 °C. Later, the solution was electrospun using a Fluidnatek® LE-10 lab device manufactured by Bioinicia S.L. (Valencia, Spain). The equipment was operated with a single needle injector, with a diameter of 0.9 mm, scanning horizontally towards a metal plate collector at room temperature conditions, that is, 25 °C and 40% relative humidity (RH). The optimal processing conditions were set at a flow-rate of 6 ml/h, 20 kV of voltage, and 20 cm needle-to-collector distance.

2.3. CNCs and CNC blends

The CNCs was prepared as a 2% (w/v) aqueous solution. Briefly, the CNCs powder was first immersed in water and homogenized at 15,000 rpm for 3 min with a T25 digital Ultra-turrax from IKA® (Staufen, Germany) and then magnetically stirred without temperature for at least 12 h. In addition, several nanocomposite solutions of the protein and three polysaccharides containing CNCs were also prepared as previously described by Reddy and Rhim (Reddy & Rhim, 2014). To this end, water solutions with total solid contents of 2% (w/v) were similarly prepared, where 98% (w/w) correspond to the biopolymers, that is, GE, AG, XG, and GA, and 2% (w/w) to CNCs. In these biopolymer solutions, 1 wt% of glycerol was added as a plasticizer, replacing the same quantity of water.

2.4. Solution properties

The viscosity, surface tension, and conductivity for all the solutions prepared above was measured. The apparent viscosity (ηa) was determined at 100 s^{-1} using a rotational viscosity meter Visco BasicPlus L from Fungilab S.A. (San Feliu de Llobregat, Spain) equipped with a low-viscosity adapter (LCP). The surface tension was measured following the Wilhemy plate method using an EasyDyne K20 tensiometer from Krüss GmbH (Hamburg, Germany). The conductivity was evaluated using a conductivity meter XS Con6 from Lab-box (Barcelona, Spain). All measurements were carried out at room temperature in triplicate.

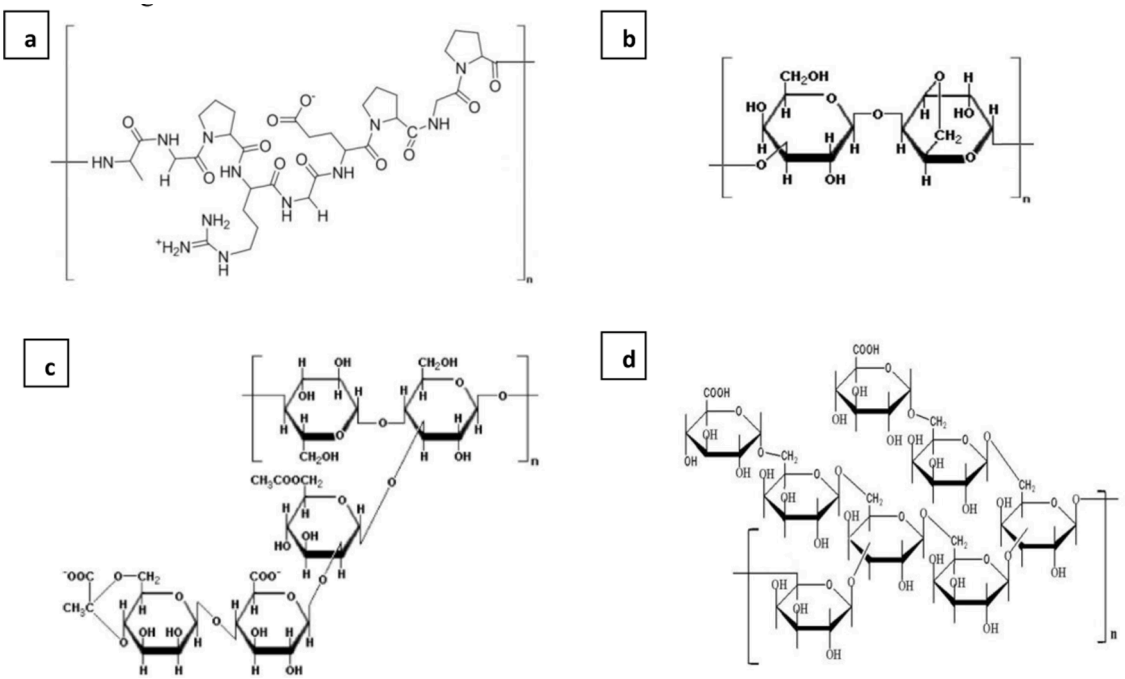

Fig. 1. Scheme of the chemical structures of: (a) Gelatin (GE); (b) Agar (AG); (c) Xanthan gum (XG); (d) Gum arabic (GA).

2.5. Preparation of the multilayers

The CNCs and the biocomposites with CNCs were impregnated onto the commercial electrospun PHBV fibers mat using the K Control Coater standard K101 model from RK PrintCoat Instruments Ltd (Litlington, UK). The roll number used was 8. The impregnation process was carried out two times. After the first application, the impregnation was dried in the oven at 90 °C for 10 min, and after the second impregnation, this was dried also at 90 °C but for 15 min. By drying at 90 °C, the electrospun nanofiber morphology of PHBV was not affected, in agreement with previous studies (Melendez-Rodriguez et al., 2018, 2020).

To generate the continuous multilayers, the electrospun PHBV substrates with no impregnation, and impregnated with CNCs and with CNCs and the hydrocolloids were sandwiched with similar non-impregnated layers of electrospun PHBV fibers and annealed at 160 °C for 2 s, without pressure, in a 4122-model press from Carver, Inc. (Wabash, IN, USA). Annealing of the PHBV at 160 °C, below the PHBV's melting point, is known from previous works to lead to continuous layers by a process of interfiber coalescence (Figueroa-Lopez, Cabedo, Lagaron & Torres-Giner, 2020a). The average thickness of the resultant multilayer biopapers was approximately 100 μm. The schemes of these assemblies are shown in Fig. 2. The samples were stored in a desiccator at 0% RH for at least 2 weeks before subsequent characterization.

2.6. Characterization

2.6.1. Scanning electron microscopy

The surface morphology of the neat and impregnated PHBV fibers and the cross-sections of the multilayer biopapers were observed by scanning electron microscopy (SEM) using an S-4800 device from Hitachi (Tokyo, Japan). For cross-section observation, the multilayers were cryo-fractured by immersion in liquid nitrogen and, then, fixed to beveled holders using conductive double-sided adhesive tape and sputtered with a mixture of gold-palladium under vacuum prior to observation. An accelerating voltage of 10 kV was used and the estimation of the dimensions was performed by means of the Aperture software from Apple (Cupertino, CA, USA) using a minimum of 20 SEM micrographs in their original magnification.

2.6.2. Mechanical tests

Tensile tests on the multilayer biopapers were performed according to ASTM standard method D638 using a 4400 universal testing machine from Instron (Norwood, MA, USA) equipped with a 1-kN load cell. The tests were performed with 115 mm × 16 mm stamped dumb-bell shaped specimens. Samples were conditioned at 40% RH and 25 °C for 24 h prior to tensile assay. A minimum of six specimens were measured for each sample, at room conditions, using a cross-head speed of 10 mm/min.

2.6.3. Barrier properties

The water vapor permeance (WVP) of the multilayer biopapers was determined using the gravimetric method ASTM E96–95 in triplicate. The control samples were cups with aluminum films to estimate solvent loss through the sealing. For this, 5 ml of distilled water was placed inside a Payne permeability cup (diameter of 3.5 cm) from Elcometer Sprl (Hermallesous-Argenteau, Belgium). The multilayers were not in direct contact with water but exposed to 100% RH on one side and secured with silicon rings. They were placed within a desiccator, sealed with dried silica gel, at 0% RH cabinet at 25 °C. WVP was calculated from the regression analysis of weight loss data vs. time, and the weight loss was calculated as the total loss minus the loss through the sealing.

For limonene permeance (LP), the procedure was similar to that described above for WVP with the difference that 5 ml of $_{D}$-limonene was placed inside the Payne permeability cups and these were placed under controlled room conditions of 25 °C and 40% RH.

The oxygen permeance (OP) coefficient was derived from the oxygen transmission rate (OTR) measurements that were recorded using an Oxygen Permeation Analyzer M8001 from Systech Illinois (Thame, UK) at 20% RH and 25 °C, in duplicate. The humidity equilibrated samples were purged with nitrogen, before exposure to an oxygen flow of 10 ml/min. The exposure area during the test was 5 cm^2 for each sample.

2.7. Statistical analysis

The mechanical and barrier properties were evaluated through analysis of variance (ANOVA) using STATGRAPHICS Centurion XVI v 16.1.03 from StatPoint Technologies, Inc. (Warrenton, VA, USA). Fisher's least significant difference (LSD) was used at the 95% confidence level ($p < 0.05$). Mean values and standard deviations were also reported.

3. Results and discussion

3.1. Solution properties and morphology

The solutions of pure CNCs and of their biocomposites with GE, AG, XG, and GA were characterized in terms of viscosity, surface tension, and conductivity, and the results are gathered in Table 1. From this

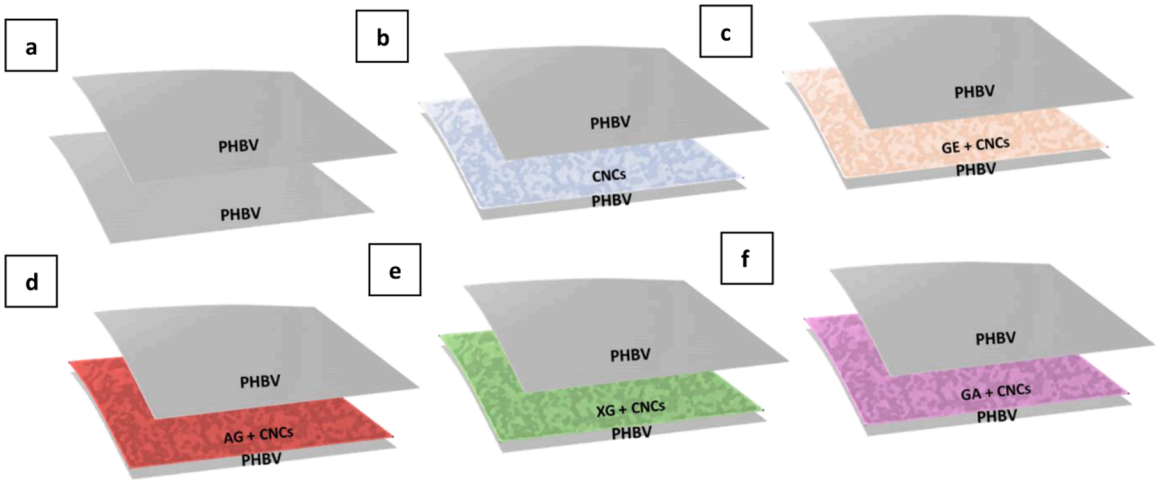

Fig. 2. Scheme of the multilayer biopapers of: (a) neat poly(3-hydroxybutyrate-*co*-3-hydroxyvalerate (PHBV); (b) PHBV impregnated with cellulose nanocrystals (CNCs); (c) PHBV impregnated with CNCs and gelatin (GE); (d) PHBV impregnated with CNCs and agar (AG); (e) PHBV impregnated with CNCs and xanthan gum (XG); and (f) PHBV impregnated with CNCs and gum arabic (GA).

Table 1
Solution properties of the neat cellulose nanocrystals (CNCs) and modified CNCs with gelatin (GE), agar (AG), xanthan gum (XG), and gum arabic (GA).

Solution	Viscosity (cP)	Surface tension (mN/m)	Conductivity (μS/cm)
CNCs	15.1 ± 0.6^{a}	49.9 ± 0.1^{a}	195.0 ± 6.1^{a}
GE with CNCs	5.2 ± 1.5^{b}	47.8 ± 1.6^{a}	356.4 ± 28.8^{b}
AG with CNCs	1.9 ± 0.3^{c}	55.9 ± 0.5^{b}	1554.1 ± 33.8^{c}
XG with CNCs	939.2 ± 2.2^{d}	76.1 ± 0.1^{c}	1631.5 ± 21.9^{d}
GA with CNCs	9.6 ± 2.1^{e}	60.4 ± 0.7^{d}	368.6 ± 26.6^{b}

a–e Different letters in the same column indicate a significant difference among the samples ($p < 0.05$).

table, it can be seen that the solutions gave quite different results depending on the biopolymers. The neat CNC solution showed values of 15.1 cP, 49.9 mN/m, and 195.0 μS/cm, for viscosity, surface tension, and conductivity, respectively. Regarding the nanocomposites, XG presented the highest values in all the three properties, that is, 939.2 cP for viscosity, 76.1 mN/m for surface tension, and 1631.5 μS/cm for conductivity. The high viscosity value suggests that this polysaccharide potentially shows a higher M_W and also to the stronger interaction of the carboxyl groups (–COO–) and ether group (–C–O–C–), shown in previous Fig. 1, with the terminal hydroxyl groups (OH–) of PHBV and cellulose. The blends with GE and GA showed certain similar values, ranging between 5.2–9.6 cP, 47.8–60.4 mN/m and 356.4–368.6 μS/cm for viscosity, surface tension, and conductivity, respectively, which, as suggested by their chemical structure, points to a moderate interaction with PHBV/CNC composite. Finally, the biocomposite solution with AG presented values of 1.9 cP, 55.9 mN/m, and 1554.1 μS/cm, for viscosity, surface tension, and conductivity. The latter values can be ascribed to the lack of chemical interactions of this hydrocolloid with the biocomposite.

The morphologies of the PHBV electrospun surfaces impregnated with and without CNCs and with their biocomposites with the hydrocolloids, as well as the cross-section of the multilayers after the thermal post-treatment of annealing, were observed by SEM and the images are presented in Fig. 3. In Fig. 3a one can observe the top view of the neat electrospun PHBV mats obtained after electrospinning and the cryo-fracture surfaces of the PHBV multilayer obtained after annealing. The electrospun mat without thermal post-treatment showed the occurrence of ultrathin fibers with mean diameters of 0.92 ± 0.11 μm. After annealing, below the biopolyester melting point, a continuous biopaper with a homogeneous surface and no apparent porosity was formed by coalescence of interfibers in agreement with our previous study (Melendez-Rodriguez et al., 2018).

Fig. 3b shows the surface of the electrospun PHBV mats after CNCs impregnation. The main characteristics of the CNC solution used were a relatively low surface tension and conductivity and relatively high viscosity in comparison with the CNCs solutions containing the hydrocolloids. It has been reported that the viscosity of CNCs depends on factors such as particle concentration and aspect ratio, as well as particle size and surface area (Moberg et al., 2017; Qiao, Chen, Zhang & Yao, 2016). From this figure, an efficient impregnation of the fibers was seen, since the porosity of the mat at the surface was very much reduced. The cross-section of the multilayer biopaper also showed a continuous non-porous morphology. Moreover, the presence of the CNCs, interphasing between the two electrospun layers, could be easily discerned. This irregular CNC interphase could be the result of the densification suffered by the fibers during the interfiber coalescence process. Other researchers have reported before the way the CNCs can suitably cover the surface of substrate fibers, such as paper or polyethersulfone (PES) membranes, transitioning this to a smoother morphology (Aguilar-Sanchez et al., 2021; Gicquel, Martin, Garrido Yanez & Bras, 2017). The good impregnation properties of CNCs have been ascribed before to secondary forces via hydrogen bonding to itself, so-called self--association, and to the polymer matrix of PES membranes (Bai et al., 2020).

The impregnation of PHBV with the hydrocolloid/CNC composites showed a different behavior depending on the hydrocolloid used. For XG, and to a significant extent for AG, in Fig. 3d and e it can be respectively observed that a somewhat better fiber impregnation was produced. These differences can be explained in terms of the solution viscosity values reported above. However, in all the cases, the cross-section of their multilayers showed a compact structure, with not so

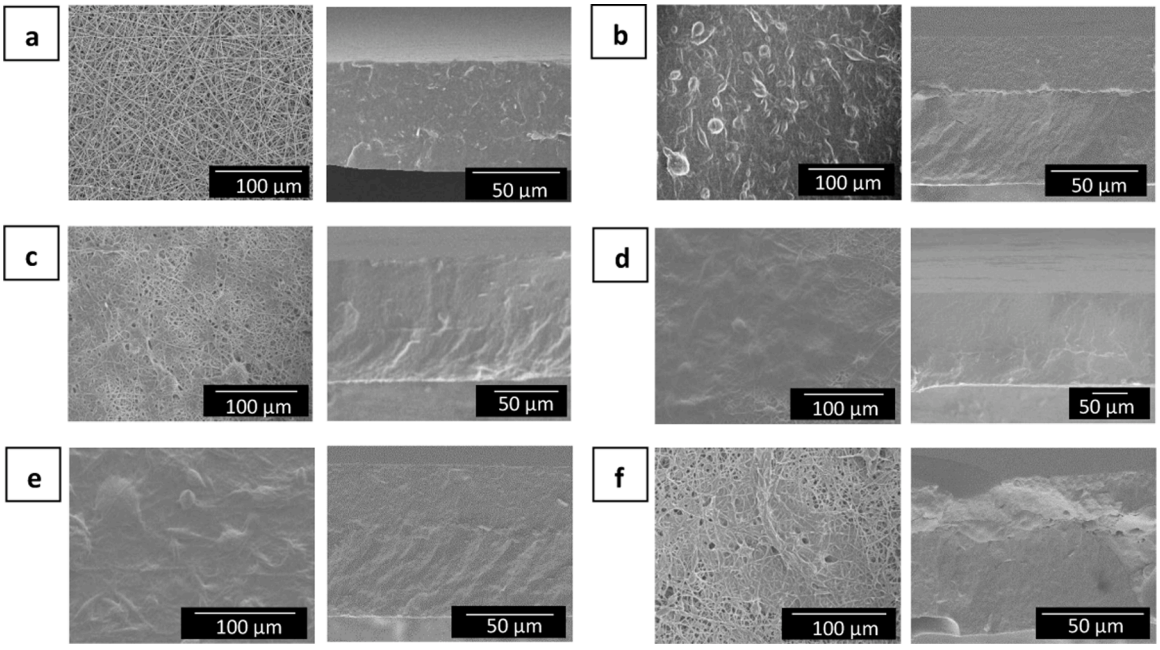

Fig. 3. Scanning electron microscopy (SEM) images of the top view of the fiber mats (left) and cross-section of the multilayers after thermal post-treatment (right) of: (a) neat poly(3-hydroxybutyrate-*co*-3-hydroxyvalerate) (PHBV); (b) PHBV impregnated with cellulose nanocrystals (CNCs); (c) PHBV impregnated with gelatin (GE) and CNCs; (d) PHBV impregnated with agar (AG) and CNCs; (e) PHBV impregnated with xanthan gum (XG) and CNCs; and (f) PHBV impregnated with gum arabic (GA) and CNCs. The images were taken at 1000x and 400x with scale markers of 50 μm and 100 μm, respectively.

clear interphase between layers after annealing, when compared to the biopaper of CNCs without hydrocolloids. The GE and GA-containing nanocomposite biopapers, respectively shown in Fig. 3c and f, indicated a less efficient impregnation of the fibers, leaving significant porosity. After annealing, they also presented homogeneous surfaces with no apparent interphase between layers. By looking at Fig. 3 and the values gathered in Table 1, it appears that the best impregnation, resulting in efficient coating of the interfibers porosity, was seen for the materials prepared with the PHBV solutions with the highest viscosity values, that is, CNCs and specially CNCs/XG. The rest of the solutions could perhaps diffuse more easily through the interfibers porosity. Penetration between the electrospun fibers depends on both the porosity of the substrate and the concentration and viscosity of the impregnation solution, as well as the impregnation process, making it difficult to predict the resulting final structure (Desmaisons, Rueff, Bras & Dufresne, 2018; Lavoine, Desloges, Khelifi & Bras, 2014).

3.2. Mechanical properties

The requirements of the multilayer materials used in packaging applications are mainly its mechanical resistance and flexibility as well as sealability. For this reason, the mechanical properties of the multilayers were assessed by tensile measurements. Table 2 shows the results of the tensile test in terms of elastic modulus (E), tensile strength at yield (σ_y), and elongation at break (ε_b). The most representative tensile stress-strain curves obtained for each multilayer at room temperature are gathered in Fig. 4. One can observe that all the multilayer materials exhibited a stiff and brittle behavior similar to the control multilayer of PHBV/PHBV. It can be seen that the multilayers of PHBV and with CNCs, that is, PHBV/CNCs/PHBV, performed almost equally in terms of E and ε_b with values around 3660 MPa and 1.3%, respectively. Regarding tensile strength, the PHBV multilayer with CNCs showed slightly lower values, not statistically significant though, than the control PHBV multilayer. Thus, the PHBV multilayer exhibited values of 26.3 MPa, while with the incorporation of CNCs the values dropped to 24.2 MPa. These slight differences in σ_y when adding a layer of nanocellulose between two layers of electrospun PHBV have been previously reported and ascribed to layer delamination at high stress. Thus, Cherpinski et al. (Cherpinski et al., 2018) obtained values of 2014.9 MPa, 28.0 MPa, and 2.8%, for E, σ_y, and ε_b, respectively, for an electrospun PHBV film monolayer, while for a multilayer made of PHBV/CNFs/ PHBV the values obtained were 2056.7 MPa, 21.0 MPa and 5.9% for E, σ_y and ε_b, respectively.

Concerning the composites based on PHBV with CNCs and hydrocolloids, it can be seen that all the multilayers presented a quite similar ε_b, ranging between 1.1–1.3%, and in the same trend as the multilayer of neat PHBV and with only CNCs. Although the multilayers with different formulations presented lower performances in relation to E, the values were also in the same range as for the control sample and with CNCs, that is, 2972–3591 MPa. Similarly, the σ_y values remained close to those

Table 2
Mechanical properties in terms of elastic modulus (E), tensile strength at yield (σ_y), and elongation at break (ε_b) of the multilayers of poly(3-hydroxybutyrate-*co*-3-hydroxyvalerate) (PHBV) with and without interlayers of cellulose nanocrystals (CNCs) and modified CNCs with gelatin (GE), agar (AG), xanthan gum (XG), and gum arabic (GA).

Multilayer	E (MPa)	σ_y (MPa)	ε_b (%)
PHBV/PHBV	3676 ± 597[a]	26.3 ± 7.6[a]	1.2 ± 0.1[a]
PHBV/CNCs/PHBV	3636 ± 820[a]	24.2 ± 6.0[a]	1.3 ± 0.2[a]
PHBV/CNCs+GE/PHBV	3536 ± 508[a]	25.0 ± 3.0[a]	1.2 ± 0.1[a]
PHBV/CNCs+AG/PHBV	3591 ± 463[a]	27.8 ± 4.7[a]	1.1 ± 0.2[a]
PHBV/CNCs+XG/PHBV	2972 ± 822[a]	21.9 ± 6.8[a]	1.2 ± 0.1[a]
PHBV/CNCs+GA/PHBV	3397 ± 860[a]	24.4 ± 5.5[a]	1.3 ± 0.3[a]

[a] Different letter in the same column indicate a significant difference among the samples ($p < 0.05$).

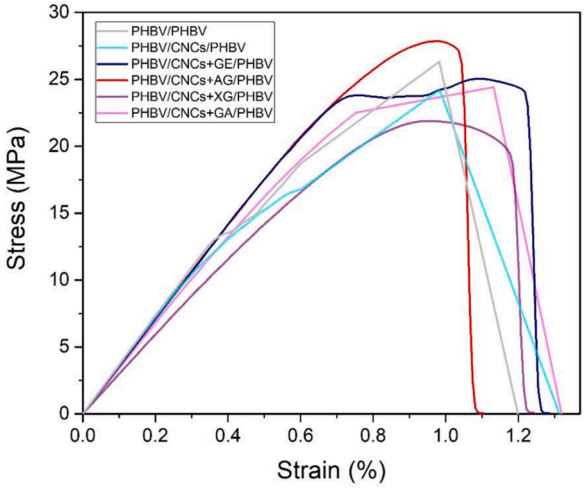

Fig. 4. Typical tensile stress–strain curves of the multilayers composed of: poly (3-hydroxybutyrate-*co*-3-hydroxyvalerate) (PHBV); PHBV with cellulose nanocrystal (CNCs); PHBV with CNCs and gelatin (GE); PHBV with CNCs and agar (AG); PHBV with CNCs and xanthan gum (XG); and PHBV with CNCs and gum arabic (GA).

achieved by the multilayers of the PHBV control and with CNCs, ranging between 21.9–27.8 MPa. The effect of CNCs addition on the mechanical performance of polymer films has been previously studied (Fox et al., 2012; Peresin et al., 2010; Shojaeiarani & Bajwa, 2018), reporting that the nanocrystals induced a stiffening effect for an optimum concentration. Thus, it has been previously reported that CNCs contents up to 7 wt %, around the percolation threshold, in a chitosan matrix showed an improvement of σ_y and a reduction of ε_b due to the good dispersion of the nanofiller (Pereda, Dufresne, Aranguren & Marcovich, 2014). However, when that optimal value was exceeded, the opposite effect occurred. This is due to agglomeration of the CNCs, which in turn leads to a reduction in their interaction with the matrix and, thus, decreases the reinforcement but increases the ductility of the films (Abdollahi, Alboofetileh, Behrooz, Rezaei & Miraki, 2013). In the current study, it is worthy to note that CNCs were used as an impregnating material, not as an additive within the fibers. Therefore, since the comparative mass fraction of the CNCs nanofibers coating is very low, the mechanical performance of the materials is mainly dominated by the intrinsic mechanical behavior of the largest phase material in the multilayer, that is, the PHBV outer layers. In fact, it may be considered as a favorable result that the properties of the modified multilayers did not get worse than the control PHBV sample, suggesting a good adhesion among the layers.

3.3. Barrier properties

Since limonene is considered a standard system for testing aroma barrier in food packaging, and oxygen and moisture permeation can dramatically detriment food shelf-life, the permeance of the multilayers based on PHBV, CNCs, and CNCs with hydrocolloids to these vapors and gas were measured. The WVP, LP, and OP values are gathered in Table 3.

In terms of WVP, it can be seen that the PHBV/PHBV multilayer showed higher barrier than the multilayer of PHBV with pure CNCs, with values of 6.0 and 24.1 $\times$ 10^{-11} kg•m^{-2}•Pa^{-1}•s^{-1}, respectively. This result can be related to the fact that it has been reported before that CNCs do not confer significant water barrier performance, even as interlayers, since the nanomaterial is hydrophilic in nature (Kelly J. Figueroa-Lopez, Sergio Torres-Giner, et al., 2020). In the latter study, however, a slight improvement in water barrier was seen since the CNCs layer was applied as a coating sandwiched between continuous and smooth layers of PHBV produced by film blowing, being pre-activated to enhance adhesion with corona treatment and pre-coated with a primer

Table 3
Thickness and permeance values in terms of water vapor permeance (WVP), D-limonene permeance (LP), and oxygen permeance (OP) of the multilayers of poly (3-hydroxybutyrate-*co*-3-hydroxyvalerate) (PHBV) with and without interlayers of cellulose nanocrystals (CNCs) and modified CNCs with gelatin (GE), agar (AG), xanthan gum (XG), and gum arabic (GA).

Multilayer	Thickness (mm)	Permeance WVP x 10^{11} (kg•m^{-2}•Pa^{-1}•s^{-1})	LP x 10^{11} (kg•m^{-2}•Pa^{-1}•s^{-1})	OP x 10^{16} (m^3•m^{-2}•Pa^{-1}•s^{-1})
PHBV/PHBV	0.097 ± 0.002	6.04 ± 2.53^{a}	2.98 ± 0.30^{a}	3.60 ± 0.60^{a}
PHBV/CNCs/PHBV	0.100 ± 0.005	24.12± 5.94^{b}	1.53 ± 0.49^{b,d}	0.42 ± 0.17^{b}
PHBV/CNCs+GE/PHBV	0.108 ± 0.007	5.18 ± 0.53^{a}	2.61 ± 0.34^{a}	23.08 ± 0.33^{c}
PHBV/CNCs+AG/PHBV	0.106 ± 0.004	19.84 ± 5.97^{b}	0.90 ± 0.21^{b,c}	7.81 ± 1.10^{d}
PHBV/CNCs+XG/PHBV	0.108 ± 0.003	10.30 ± 5.90^{a,b}	0.50 ± 0.10^{c}	2.57 ± 0.77^{a}
PHBV/CNCs+GA/PHBV	0.109 ± 0.004	7.57 ± 1.86^{a,b}	1.82 ± 0.14^{d}	2.42 ± 1.10^{a}

a-d Different letters in the same column indicate a significant difference among the samples ($p < 0.05$).

and a wetting agent. Likewise, the multilayers of CNCs with AG and XG exhibited also poorer barrier to water, showing values of 19.8 and 10.3 × 10^{-11} kg•m^{-2}•Pa^{-1}•s^{-1}, respectively, probably due to their hydrophilic nature and higher porosity. Furthermore, the samples with GE and GA retained a similar WVP as the non-impregnated multilayer, with WVP values of 5.2 and 7.6 × 10^{-11} kg•m^{-2}•Pa^{-1}•s^{-1}, respectively.

Regarding aroma barrier, the multilayer of PHBV with CNCs exhibited better barrier than the neat PHBV multilayer, showing values of 1.5 and 2.9 × 10^{-11} kg•m^{-2}•Pa^{-1}•s^{-1}, respectively. This can be explained by the fact that limonene is a strong plasticizer for PHA materials, but this is not the same for hydrophilic materials, such as CNCs, that can offer a good barrier to the permeant (Sanchez-Garcia, Gimenez & Lagaron, 2007). It has been reported a limonene uptake of up to 13 wt % for a solvent-cast PHBV film (Sanchez-Garcia, Gimenez & Lagaron, 2008). The multilayers containing the CNCs interlayer with GE and GA showed somewhat improved barrier values, that is, 2.6 and 1.8 × 10^{-11} kg•m^{-2}•Pa^{-1}•s^{-1}, respectively; whereas the samples with AG and XG, exhibited the best barrier to limonene vapor, with permeance reductions between 70 and 83% compared to the control, that is, 0.9 and 0.5 × 10^{-11} kg•m^{-2}•Pa^{-1}•s^{-1}, respectively. These two multilayer samples, specially the one containing XG, and also the one based on only CNCs, exhibited in previous Fig. 3 the best impregnation in terms of reduced porosity.

Regarding the permeance of the small non-condensable gas oxygen molecule, the sample with only CNCs showed clearly lower OP, with a reduction of 88%, than the control PHBV bilayer sample. This OP reduction value is in good agreement with previous studies in which CNCs were used as a continuous interlayer coating. For instance, Le Gars et al. (Le Gars et al., 2020) reported a nearly 90% permeation decrease in multilayers of polylactide (PLA) and CNCs (PLA/CNC/PLA). In another study, Fotie et al. (Fotie et al., 2020) studied multilayers of polyethylene terephthalate (PET), PLA, oriented polypropylene (OPP), PP, and PE with 1 μm of a continuous CNCs interlayer applied by lamination, reporting in all cases an OP reduction between 90 and 100%. It is, therefore, very interesting to see that CNCs can also achieve a very high-barrier effect, even when impregnated over electrospun mats, which upon annealing suffer a significant shrinkage during fiber coalescence. It is also inferred from the good oxygen barrier results that this interesting interfiber coalescence process, unique to electrospun biopapers, can reduce the free volume, creating a high-barrier continuous interphase. Concerning the multilayer of PHBV with CNCs and XG or GA, these samples showed a similar but slightly higher barrier performance as the control multilayer, with values of 2.6 and 2.4 × 10^{-16} m^3•m^{-2}•Pa^{-1}•s^{-1}, respectively. However, the samples with GE and AG showed the worst performance in barrier, with values of 23.1 and 7.8 × 10^{-16} m^3•m^{-2}•Pa^{-1}•s^{-1}, respectively. These last two samples exhibited in Fig. 3 the least favorable impregnation morphology. Since no oxygen barrier, driven by diffusion, was seen even for the multilayers containing the most favorable polysaccharides in terms of interphase morphology, but they presented aroma barrier, driven by solubility, it is possible that these hydrocolloids are not able to stablish a continuous interphase between the layers, further supported by the morphology data in Fig. 3.

4. Conclusions

In this study, various multilayered films composed of two electrospun PHBV fiber layers, one of which was impregnated with CNCs and hydrocolloids with CNCs, were prepared and characterized. To obtain the nanocomposites, the nanocellulose was mixed in a 2% (w/w) with a protein, GE, and three polysaccharides, AG, XG, and GA, whereas glycerol was added in all the formulations as a plasticizer. The multilayers were post-processed by a mild thermal treatment at 160 °C for 2 s, to obtain a fiber-based continuous structure. The morphology, mechanical properties, assessed via tensile tests, and barrier properties, measured in terms of permeance to water and limonene vapors and oxygen gas, of the multilayers were reported. SEM images showed that the best impregnation of the PHBV fibers was achieved with CNCs and, to a lesser extent, with their biocomposites with AG and XG. After annealing below the PHBV's melting point, all the multilayers showed good interlayer adhesion, with the layers adhering properly and showing no voids or gaps. The impregnation with neat CNCs and CNCs with hydrocolloids did not affect the mechanical properties of pure PHBV, which were found to be governed by the mechanical response of the outer structural layers of PHBV, but their barrier properties to limonene were improved in all the cases, especially, with CNCs and their biocomposites with AG and XG. The oxygen permeance was seen to be largely improved only after impregnation with CNCs. The results showed, therefore, that the best impregnation material in terms of the properties analyzed, with the exception of the water permeance, corresponded to CNCs. Some of the hydrocolloid nanocomposites with the best impregnation morphology showed only improvements in aroma barrier.

Credit authorship contribution statement

Beatriz Melendez-Rodriguez: Investigation, Validation, Writing – original draft. **Marie-Stella M'Bengue:** Methodology, Investigation, Validation, Writing – original draft. **Sergio Torres-Giner:** Supervision, Writing – review & editing. **Luis Cabedo:** Investigation, Validation. **Cristina Prieto:** Writing – review & editing, Supervision. **Jose Maria Lagaron:** Conceptualization, Resources, Validation, Writing – review & editing.

Funding

This research work was funded by the H2020 EU project USABLE PAKAGING (reference number 836884) and by the Spanish Ministry of Science and Innovation (MICI) project RTI2018-097249-B-C21.

Declaration of Competing Interest

The authors declare no conflict of interest.

Acknowledgments

Ms. Beatriz Melendez-Rodriguez would like to acknowledge the MICI for her FPI fellowship (BES-2016-077972) and Dr. Torres-Giner for his MICI Juan de la Cierva–Incorporación contract (IJCI-2016-29675). The authors would also like to acknowledge the Unidad Asociada IATA (CSIC)-UJI in "Polymer Technology".

References

Abdollahi, M., Alboofetileh, M., Behrooz, R., Rezaei, M., & Miraki, R. (2013). Reducing water sensitivity of alginate bio-nanocomposite film using cellulose nanoparticles. *International Journal of Biological Macromolecules, 54*, 166–173.

Aguilar-Sanchez, A., Jalvo, B., Mautner, A., Nameer, S., Pöhler, T., Tammelin, T., et al. (2021). Waterborne nanocellulose coatings for improving the antifouling and antibacterial properties of polyethersulfone membranes. *Journal of Membrane Science, 620*, Article 118842.

Ahankari, S. S., Subhedar, A. R., Bhadauria, S. S., & Dufresne, A. (2021). Nanocellulose in food packaging: A review. *Carbohydrate Polymers, 255*, Article 117479.

Aphibanthammakit, C., Nigen, M., Gaucel, S., Sanchez, C., & Chalier, P. (2018). Surface properties of Acacia senegal vs Acacia seyal films and impact on specific functionalities. *Food Hydrocolloids, 82*, 519–533.

Atef, M., Rezaei, M., & Behrooz, R. (2014). Preparation and characterization agar-based nanocomposite film reinforced by nanocrystalline cellulose. *International Journal of Biological Macromolecules, 70*, 537–544.

Aulin, C., Gällstedt, M., & Lindström, T. (2010). Oxygen and oil barrier properties of microfibrillated cellulose films and coatings. *Cellulose (London, England), 17*(3), 559–574.

Bai, L., Ding, J., Wang, H., Ren, N., Li, G., & Liang, H. (2020). High-performance nanofiltration membranes with a sandwiched layer and a surface layer for desalination and environmental pollutant removal. *Science of The Total Environment, 743*, Article 140766.

Bhatia, S. K., Otari, S. V., Jeon, J.-. M., Gurav, R., Choi, Y.-. K., Bhatia, R. K., et al. (2021). Biowaste-to-bioplastic (polyhydroxyalkanoates): Conversion technologies, strategies, challenges, and perspective. *Bioresource Technology, 326*, Article 124733.

Cao, N., Yang, X., & Fu, Y. (2009). Effects of various plasticizers on mechanical and water vapor barrier properties of gelatin films. *Food Hydrocolloids, 23*(3), 729–735.

Chen, C. W., Don, T.-. M., & Yen, H.-. F. (2006). Enzymatic extruded starch as a carbon source for the production of poly(3-hydroxybutyrate-co-3-hydroxyvalerate) by Haloferax mediterranei. *Process Biochemistry, 41*(11), 2289–2296.

Cherpinski, A., Torres-Giner, S., Cabedo, L., Méndez, J. A., & Lagaron, J. M. (2018a). Multilayer structures based on annealed electrospun biopolymer coatings of interest in water and aroma barrier fiber-based food packaging applications. *Journal of Applied Polymer Science, 135*(24), 45501.

Cherpinski, A., Torres-Giner, S., Vartiainen, J., Peresin, M. S., Lahtinen, P., & Lagaron, J. M. (2018b). Improving the water resistance of nanocellulose-based films with polyhydroxyalkanoates processed by the electrospinning coating technique. *Cellulose (London, England), 25*(2), 1291–1307.

Clarke, D., Molinaro, S., Tyuftin, A., Bolton, D., Fanning, S., & Kerry, J. P. (2016). Incorporation of commercially-derived antimicrobials into gelatin-based films and assessment of their antimicrobial activity and impact on physical film properties. *Food control, 64*, 202–211.

Commission, E. (2018). Plastic Waste: A European strategy to protect the planet, defend our citizens and empower our industries, accessed 2021. https://ec.europa.eu/commission/presscorner/detail/en/IP_18_5.

Desmaisons, J., Rueff, M., Bras, J., & Dufresne, A. (2018). Impregnation of paper with cellulose nanocrystal reinforced polyvinyl alcohol: Synergistic effect of infrared drying and CNC content on crystallinity. *Soft matter, 14*(46), 9425–9435.

Doshi, J., & Reneker, D. H. (1995). Electrospinning process and applications of electrospun fibers. *Journal of Electrostatics, 35*(2), 151–160.

Fabra, M. J., López-Rubio, A., Ambrosio-Martín, J., & Lagaron, J. M. (2016). Improving the barrier properties of thermoplastic corn starch-based films containing bacterial cellulose nanowhiskers by means of PHA electrospun coatings of interest in food packaging. *Food Hydrocolloids, 61*, 261–268.

Figueroa-Lopez, K. J., Cabedo, L., Lagaron, J. M., & Torres-Giner, S. (2020a). Development of Electrospun Poly(3-hydroxybutyrate-co-3-hydroxyvalerate) Monolayers Containing Eugenol and Their Application in Multilayer Antimicrobial Food Packaging. *Frontiers in Nutrition, 7*(140).

Figueroa-Lopez, K. J., Enescu, D., Torres-Giner, S., Cabedo, L., Cerqueira, M. A., Pastrana, L., et al. (2020b). Development of electrospun active films of poly(3-hydroxybutyrate-co-3-hydroxyvalerate) by the incorporation of cyclodextrin inclusion complexes containing oregano essential oil. *Food Hydrocolloids, 108*, Article 106013.

Figueroa-Lopez, K. J., Torres-Giner, S., Angulo, I., Pardo-Figuerez, M., Escuin, J. M., Bourbon, A. I., et al. (2020c). Development of active barrier multilayer films based on electrospun antimicrobial hot-tack food waste derived poly(3-hydroxybutyrate-co-3-hydroxyvalerate) and cellulose nanocrystal interlayers. *Nanomaterials, 10*(12), 2356.

Fotie, G., Gazzotti, S., Ortenzi, M. A., & Piergiovanni, L. (2020). Implementation of high gas barrier laminated films based on cellulose nanocrystals for food flexible packaging. *Applied Sciences, 10*(9), 3201.

Fox, J., Wie, J. J., Greenland, B. W., Burattini, S., Hayes, W., Colquhoun, H. M., et al. (2012). High-strength, healable, supramolecular polymer nanocomposites. *Journal of the American Chemical Society, 134*(11), 5362–5368.

Gallardo-Cervantes, M., González-García, Y., Pérez-Fonseca, A. A., González-López, M. E., Manríquez-González, R., Rodrigue, D., et al. (2021). Biodegradability and improved mechanical performance of polyhydroxyalkanoates/agave fiber biocomposites compatibilized by different strategies. *Journal of Applied Polymer Science, 138*(15), 50182.

Ge, H., Wu, Y., Woshnak, L. L., & Mitmesser, S. H. (2021). Effects of hydrocolloids, acids and nutrients on gelatin network in gummies. *Food Hydrocolloids, 113*, Article 106549.

Geyer, R., Jambeck, J. R., & Law, K. L. (2017). Production, use, and fate of all plastics ever made. *Science Advances, 3*(7), Article e1700782.

Gicquel, E., Martin, C., Garrido Yanez, J., & Bras, J. (2017). Cellulose nanocrystals as new bio-based coating layer for improving fiber-based mechanical and barrier properties. *Journal of Materials Science, 52*(6), 3048–3061.

Gómez-Guillén, M. C., Pérez-Mateos, M., Gómez-Estaca, J., López-Caballero, E., Giménez, B., & Montero, P. (2009). Fish gelatin: A renewable material for developing active biodegradable films. *Trends in Food Science & Technology, 20*(1), 3–16.

Guk Choi, G., Woong Kim, M., Kim, J.-. Y., & Ha Rhee, Y. (2003). Production of poly(3-hydroxybutyrate-co-3-hydroxyvalerate) with high molar fractions of 3-hydroxyvalerate by a threonine-overproducing mutant of Alcaligenes sp. SH-69. *Biotechnology Letters, 25*(9), 665–670.

Guo, J., Ge, L., Li, X., Mu, C., & Li, D. (2014). Periodate oxidation of xanthan gum and its crosslinking effects on gelatin-based edible films. *Food Hydrocolloids, 39*, 243–250.

Montenegro, M., Boiero, L., Valle, L., & Borsarelli, C. (2012). *Gum Arabic: More Than an Edible Emulsifier*. In Products and Applications of Biopolymers. *IntechOpen*.

Nur Hanani, Z. A., Roos, Y. H., & Kerry, J. P. (2012). Use of beef, pork and fish gelatin sources in the manufacture of films and assessment of their composition and mechanical properties. *Food Hydrocolloids, 29*(1), 144–151.

Hubbe, M. A., Ferrer, A., Tyagi, P., Yin, Y., Salas, C., Pal, L., et al. (2017). Nanocellulose in Thin Films, Coatings, and Plies for Packaging Applications: A Review. *Bioresources, 12(1)*(91), 2143–2233. *2017*.

Huber, T., Müssig, J., Curnow, O., Pang, S., Bickerton, S., & Staiger, M. P. (2012). A critical review of all-cellulose composites. *Journal of Materials Science, 47*(3), 1171–1186.

Jansson, P.-e., Kenne, L., & Lindberg, B. (1975). Structure of the extracellular polysaccharide from xanthomonas campestris. *Carbohydrate Research, 45*(1), 275–282.

Kang, S., Xiao, Y., Guo, X., Huang, A., & Xu, H. (2021). Development of gum arabic-based nanocomposite films reinforced with cellulose nanocrystals for strawberry preservation. *Food Chemistry, 350*, Article 129199.

Kanmani, P., & Rhim, J.-. W. (2014). Antimicrobial and physical-mechanical properties of agar-based films incorporated with grapefruit seed extract. *Carbohydrate Polymers, 102*, 708–716.

Kumar, A., Rao, K. M., & Han, S. S. (2018). Application of xanthan gum as polysaccharide in tissue engineering: A review. *Carbohydrate Polymers, 180*, 128–144.

Akshay Kumar, K. P., Zare, E. N., Torres-Mendieta, R., Wacławek, S., Makvandi, P., Černík, M., … Varma, R. S. (2021). Electrospun fibers based on botanical, seaweed, microbial, and animal sourced biomacromolecules and their multidimensional applications. *International Journal of Biological Macromolecules, 171*, 130–149.

Lavoine, N., Desloges, I., Khelifi, B., & Bras, J. (2014). Impact of different coating processes of microfibrillated cellulose on the mechanical and barrier properties of paper. *Journal of Materials Science, 49*(7), 2879–2893.

Le Gars, M., Dhuiège, B., Delvart, A., Belgacem, M. N., Missoum, K., & Bras, J. (2020). High-barrier and antioxidant poly(lactic acid)/nanocellulose multilayered materials for packaging. *ACS Omega, 5*(36), 22816–22826.

Leite, L. S. F., Ferreira, C. M., Corrêa, A. C., Moreira, F. K. V., & Mattoso, L. H. C. (2020). Scaled-up production of gelatin-cellulose nanocrystal bionanocomposite films by continuous casting. *Carbohydrate Polymers, 238*, Article 116198.

Li, X., Zhang, H., He, L., Chen, Z., Tan, Z., You, R., et al. (2018). Flexible nanofibers-reinforced silk fibroin films plasticized by glycerol. *Composites Part B: Engineering, 152*, 305–310.

Madhusudana Rao, K., Kumar, A., & Han, S. S. (2017). Polysaccharide based bionanocomposite hydrogels reinforced with cellulose nanocrystals: Drug release and biocompatibility analyses. *International Journal of Biological Macromolecules, 101*, 165–171.

Melendez-Rodriguez, B., Castro-Mayorga, J. L., Reis, M. A. M., Sammon, C., Cabedo, L., Torres-Giner, S., et al. (2018). Preparation and characterization of electrospun food biopackaging films of poly(3-hydroxybutyrate-co-3-hydroxyvalerate) derived from fruit pulp biowaste. *Frontiers in Sustainable Food Systems, 2*(38).

Melendez-Rodriguez, B., Torres-Giner, S., Lorini, L., Valentino, F., Sammon, C., Cabedo, L., et al. (2020). Valorization of municipal biowaste into electrospun poly(3-hydroxybutyrate-co-3-hydroxyvalerate) biopapers for food packaging applications. *ACS Applied Bio Materials, 3*(9), 6110–6123.

Moberg, T., Sahlin, K., Yao, K., Geng, S., Westman, G., Zhou, Q., et al. (2017). Rheological properties of nanocellulose suspensions: Effects of fibril/particle dimensions and surface characteristics. *Cellulose (London, England), 24*(6), 2499–2510.

Mokhena, T. C., & John, M. J. (2020). Cellulose nanomaterials: New generation materials for solving global issues. *Cellulose (London, England), 27*(3), 1149–1194.

Pereda, M., Dufresne, A., Aranguren, M. I., & Marcovich, N. E. (2014). Polyelectrolyte films based on chitosan/olive oil and reinforced with cellulose nanocrystals. *Carbohydrate Polymers, 101*, 1018–1026.

Peresin, M. S., Habibi, Y., Vesterinen, A.-. H., Rojas, O. J., Pawlak, J. J., & Seppälä, J. V. (2010). Effect of moisture on electrospun nanofiber composites of poly(vinyl alcohol) and cellulose nanocrystals. *Biomacromolecules, 11*(9), 2471–2477.

Qiao, C., Chen, G., Zhang, J., & Yao, J. (2016). Structure and rheological properties of cellulose nanocrystals suspension. *Food Hydrocolloids, 55*, 19–25.

Qiu, Y.-. Z., Han, J., & Chen, G.-. Q. (2006). Metabolic engineering of Aeromonas hydrophila for the enhanced production of poly(3-hydroxybutyrate-co-3-hydroxyhexanoate). *Applied Microbiology and Biotechnology, 69*(5), 537–542.

Reddy, J. P., & Rhim, J.-. W. (2014). Characterization of bionanocomposite films prepared with agar and paper-mulberry pulp nanocellulose. *Carbohydrate Polymers, 110*, 480–488.

Rhim, J. W., Wang, L. F., & Hong, S. I. (2013). Preparation and characterization of agar/silver nanoparticles composite films with antimicrobial activity. *Food Hydrocolloids, 33*(2), 327–335.

Sanchez-Garcia, M. D., Gimenez, E., & Lagaron, J. M. (2007). Novel PET nanocomposites of interest in food packaging applications and comparative barrier performance with biopolyester nanocomposites. *Journal of Plastic Film & Sheeting, 23*(2), 133–148.

Sanchez-Garcia, M. D., Gimenez, E., & Lagaron, J. M. (2008). Morphology and barrier properties of solvent cast composites of thermoplastic biopolymers and purified cellulose fibers. *Carbohydrate Polymers, 71*(2), 235–244.

Santos, T. M., Souza Filho, M.d. S. M., Caceres, C. A., Rosa, M. F., Morais, J. P. S., Pinto, A. M. B., et al. (2014). Fish gelatin films as affected by cellulose whiskers and sonication. *Food Hydrocolloids, 41*, 113–118.

Shojaeiarani, J., & Bajwa, D. (2018). Functionalized cellulose nanocrystals for improving the mechanical properties of poly(lactic acid). In *ASME 2018 International Mechanical Engineering Congress and Exposition (Vol. Volume 12: Materials: Genetics to Structures)*.

Tong, Q., Xiao, Q., & Lim, L.-. T. (2013). Effects of glycerol, sorbitol, xylitol and fructose plasticisers on mechanical and moisture barrier properties of pullulan–alginate–carboxymethylcellulose blend films. *International Journal of Food Science & Technology, 48*(4), 870–878.

Torres-Giner, S. (2011). 5 - Electrospun nanofibers for food packaging applications. In J.-M. Lagarón (Ed.), *Multifunctional and nanoreinforced polymers for food packaging* (pp. 108–125). Hoboken, New Jersey, US: Woodhead Publishing.

Torres-Giner, S., Montanes, N., Boronat, T., Quiles-Carrillo, L., & Balart, R. (2016). Melt grafting of sepiolite nanoclay onto poly(3-hydroxybutyrate-*co*-4-hydroxybutyrate) by reactive extrusion with multi-functional epoxy-based styrene-acrylic oligomer. *European Polymer Journal, 84*, 693–707.

Trache, D., Tarchoun, A. F., Derradji, M., Hamidon, T. S., Masruchin, N., Brosse, N., et al. (2020). Nanocellulose: From Fundamentals to Advanced Applications. *Frontiers in Chemistry, 8*(392).

Verbeken, D., Dierckx, S., & Dewettinck, K. (2003). Exudate gums: Occurrence, production, and applications. *Applied Microbiology and Biotechnology, 63*(1), 10–21.

Wang, J., Gardner, D. J., Stark, N. M., Bousfield, D. W., Tajvidi, M., & Cai, Z. (2018). Moisture and Oxygen Barrier Properties of Cellulose Nanomaterial-Based Films. *ACS Sustainable Chemistry & Engineering, 6*(1), 49–70.

Xiao, C., Zhang, Z., Zhang, J., Lu, Y., & Zhang, L. (2003). Properties of regenerated cellulose films plasticized with α-monoglycerides. *Journal of Applied Polymer Science, 89*(13), 3500–3505.

Zhang, H. F., Ma, L., Wang, Z. H., & Chen, G. Q. (2009). Biosynthesis and characterization of 3-hydroxyalkanoate terpolyesters with adjustable properties by Aeromonas hydrophila. *Biotechnol Bioeng, 104*(3), 582–589.

Zhao, W., & Chen, G.-. Q. (2007). Production and characterization of terpolyester poly(3-hydroxybutyrate-co-3-hydroxyvalerate-co-3-hydroxyhexanoate) by recombinant Aeromonas hydrophila 4AK4 harboring genes phaAB. *Process Biochemistry, 42*(9), 1342–1347.

Zhao, Y., Moser, C., Lindström, M. E., Henriksson, G., & Li, J. (2017). Cellulose Nanofibers from Softwood, Hardwood, and Tunicate: Preparation–Structure–Film Performance Interrelation. *ACS Applied Materials & Interfaces, 9*(15), 13508–13519.